

This is the accepted manuscript, which has been accepted by IEEE for publication © 2014. Personal use of this material is permitted. Permission from IEEE must be obtained for all other uses, in any current or future media, including reprinting/republishing this material for advertising or promotional purposes, creating new collective works, for resale or redistribution to servers or lists, or reuse of any copyrighted component of this work in other works. The full reference is:

‘Effect of Water Streams on the AC Breakdown Performance of Short Rod-plane Air Gaps’

Y. Yuan, X. Jiang, S. M. Rowland X. Cheng and Qi Li

IEEE Transactions on Dielectrics and Electrical Insulation, Vol. 21, Issue 4,
pp. 1747-1756 (2014)

Digital Object Identifier: [10.1109/TDEI.2014.004239](https://doi.org/10.1109/TDEI.2014.004239)

Effect of Water Streams on the AC Breakdown Performance of Short Rod-plane Air Gaps

Yao Yuan, Xingliang Jiang

State Key Laboratory of Power Transmission Equipment and System Security and New Technology
School of Electrical Engineering, Chongqing University
Chongqing, 400044 China

Simon M. Rowland, Xian Cheng and Qi Li

University of Manchester
School of Electrical and Electronic Engineering
Manchester, M13 9PL, UK

ABSTRACT

The ac breakdown performance of rod-plane air gaps in the presence of water streams has been explored. Experimental results show that the ac breakdown voltage of rod-plane short air gaps in the presence of a water stream is significantly lower than in the dry condition. In addition, the ac breakdown voltage of an air gap decreases with the increase of the water stream velocity, diameter and conductivity. The relative breakdown voltage of an air gap decreases with an increase of water stream velocity from 0.75 m/s to 1.79 m/s and nozzle diameter from 1.0 mm to 3.0 mm by 2.6% / 0.1 m/s and 0.8% / 0.1 mm, respectively. High speed images of the deformation of the water stream and the breakdown process of air gap are reported show that with the increase of the applied voltage, the critical break-up length and the size of main water droplets decrease. In addition, the effect of the electrical field on the break-up length of a water stream and the size of droplets are independent of the jet velocity.

Index Terms — water, stream, breakdown, air gap, rod-plane, jet, break-up, breakup, electrified

1 INTRODUCTION

IN China, lightning, pollution and icing pose a great threat to the safe operation of transmission lines. This requires the National Grid of China to pay considerable attention to the insulation of transmission lines which go through hugely varied environments. In 2009 and 2010, several trip faults were caused by heavy rain in the region of the Three-Gorges, causing severe damage to the power grid. In addition, in 2007 and 2008, a total of 89 of 35 kV lines in Chongqing and 55 of 10 kV lines, 13 of 35 kV lines and 6 of 110 kV lines in Nanchang tripped in periods of heavy rain. However, the influence of heavy rain on the breakdown of air gaps is seldom considered in the engineering design of transmission lines.

Some studies have been carried out to investigate the effect of rain on the breakdown performance of air gaps. Rizk [2-3] investigated the influence of rain on the switching impulse spark-over voltage of sphere-plane, toroid-plane and rod-plane air gaps. It was found that for the rod-plane air gap, the negative discharge voltage decreases significantly due to the effect of rain, however, the positive discharge voltage is not affected. In 2002, Yamagata [4] carried out full-scale experiments on phase-to-ground and phase-to-phase insulation with different gap lengths in dry and

wet conditions. It was shown that the critical flashover voltage under wet conditions was reduced by 8%-15% compared to tests under dry conditions. In 2008, Hu and Wang [5] studied the influence of rain and wind on power frequency discharge characteristic of conductor-to-tower air gaps. It was determined that with the increase of rain intensity and rain conductivity, the discharge voltage of conductor-to-tower air gaps decreases. Similar conclusions on ac and dc rod-plane air gap have been obtained by Jiang [6-7].

Research in [2-7] focused on the effect of water droplets on the breakdown performance of air-gaps and did not consider the water stream which can be formed at the end of electrodes under heavy rain conditions. According to the authors' results [6-7], the breakdown voltage of rod-plane air gaps will be decreased just by 5%-8% due to the effect of water droplets. It is suggested then that the effect of water droplets may not be the reason for the trip faults seen in transmission lines in periods of heavy rain. Rather it is proposed that, the formation of water streams along the conductors, fittings, and insulators can effectively shorten the insulating gaps and so pose a threat to the safe operation of transmission line systems. The authors have also illustrated one of the mechanisms by which such water flows may occur [8].

Although there is little literature related to the breakdown of air gaps in rainy conditions or water streams, the break-up performance and mechanism of a water stream or liquid jet have

been well studied. A water stream with initial constant diameter, D , falls vertically under gravity. The stream length increases and reaches to a critical value. After that, the stream breaks up and decomposes into droplets because of the effect of surface tension. This phenomenon, shown in Figure 1, was first investigated by Joseph Plateau [9], and later Lord Rayleigh gave an analytical explanation [10]-[11]. Since then, a large number of experimental and theoretical studies on the break-up phenomenon for liquid jets injected from a round nozzle have been carried out by many researchers [12-33].

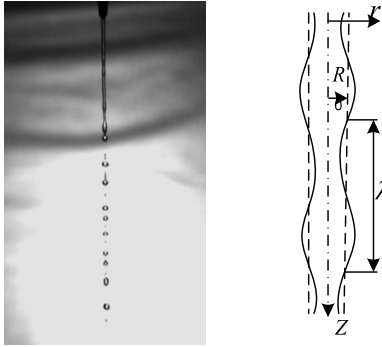


Figure 1. Plateau-Rayleigh instability jet and the theoretical model [12].

According to Rayleigh's analysis [10], the falling water jet surface varies with time and space, and the radial distance from the axis to the surface takes the form:

$$r = R_0 + \epsilon_0 e^{\omega t + ikz} \quad (1)$$

where $R_0 = D/2$; the initial perturbation amplitude $\epsilon_0 \ll R_0$; ω is the growth rate of the instability; k is the wave number and $k = 2\pi/\lambda$; λ is the wavelength shown in Figure 1.

By applying Navier-Stokes equations together with continuity equations and Young-Laplace equations [13], the dispersion relation that indicates the dependence of the growth rate ω on the wave number k can be solved as:

$$\omega^2 = \frac{\sigma}{\rho R_0^3} k R_0 \frac{I_1(kR_0)}{I_0(kR_0)} (1 - k^2 R_0^2) \quad (2)$$

where σ is the surface tension; ρ is the liquid density; I_0 and I_1 are modified Bessel functions of the first kind.

However, equation (2) does not take any effect of the electrical field into account. Thus, based on the work of Rayleigh, Son and Ohba derived a dispersion equation which accounts for the growth rate of an electrically charged liquid jet considering the needle-plane configuration by employing Lagrange's equation of motion [12]. As shown in equation (3), where ϵ_0 is the permittivity of air; k_0 and k_1 are modified Bessel functions of the second kind:

$$\omega^2 = \frac{\sigma}{\rho R_0^3} k R_0 \frac{I_1(kR_0)}{I_0(kR_0)} (1 - k^2 R_0^2) - \frac{\epsilon_0 U_0^2}{\rho R_0^4 \ln(4d/R_0)} k R_0 \frac{I_1(kR_0)}{I_0(kR_0)} \left[1 - k R_0 \frac{k_1(kR_0)}{k_0(kR_0)} \right] \quad (3)$$

As the velocity varies, the liquid jet is characterized by different break-up modes, which are shown in Figure 2. It can be seen that different break-up behavior is seen with an increase of jet velocity. Figure 3 illustrates the relationship between break-up length and velocity of the liquid jet. In the

Rayleigh regime, the break-up length of a liquid jet has a linearly relationship with jet velocity. According to Sterling's experiment results [16], the critical velocity of a water stream, distinguishing the Rayleigh regime and first wind induced break-up regime, v_{c2} is 2.2 m/s.

In natural rain conditions, the water column formed along an insulator string is mainly affected by gravity and thus its velocity will not be high. Therefore, in this paper, we have mainly investigated the effect of water streams within the Rayleigh regime. The influence of velocity and radius of the water stream has been analyzed and the spatial distortion of the water stream with the applied voltage has also been studied by using a high speed camera.

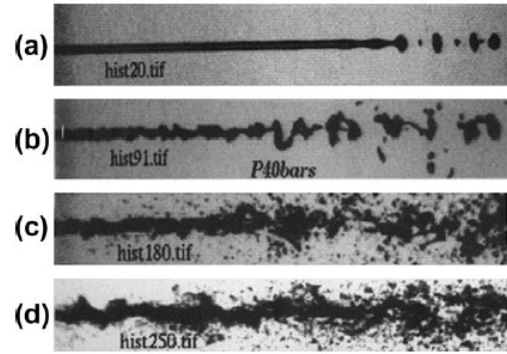


Figure 2. Disintegration regimes (a: Rayleigh breakup mode, b: first wind induced, c: second wind induced, d: atomization mode) [14].

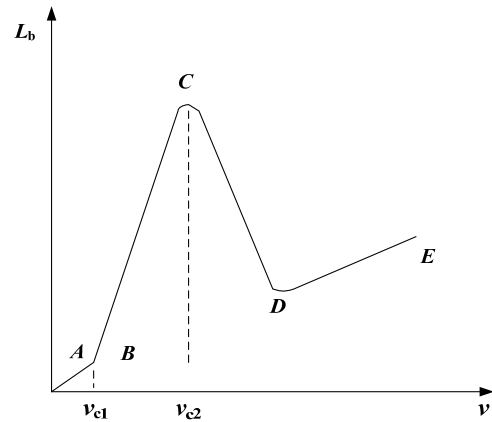


Figure 3. Relationship between break-up length and velocity of liquid jet (AB-dripping regime, BC-Rayleigh regime, CD-first wind induced break-up regime, DE-second wind induced break-up regime) [15].

2 TEST ARRANGEMENTS AND METHODS

The tests were carried out in the University of Manchester National Grid High Voltage Research Centre Laboratory. In all of the tests, the rod-plane air gap was arranged with the rod vertical. The nozzle electrode was made of brass and shaped as shown in Figure 4, where $L_1=L_2=3.0$ cm, $D_1=11.9$ mm, $D_2=6.0$ mm, D was set to =1.0, 1.5, 2.0, 2.5 and 3.0 mm because in practice typical raindrops have diameters between 1 and 3 mm. Drop sizes above 8 mm have been observed but they become unstable and readily break up due to surface tension [17]. For the plane electrode, a 0.5 m \times 3.0 m rectangle of galvanized 1.0 mm thick iron plate was used. The radius of curvature on

the internal and external diameters at the nozzle openings was $2/D$ and $2/D_2$.

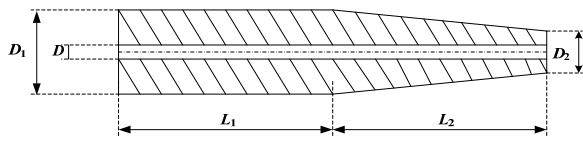


Figure 4. Schematic diagram of nozzle electrode.

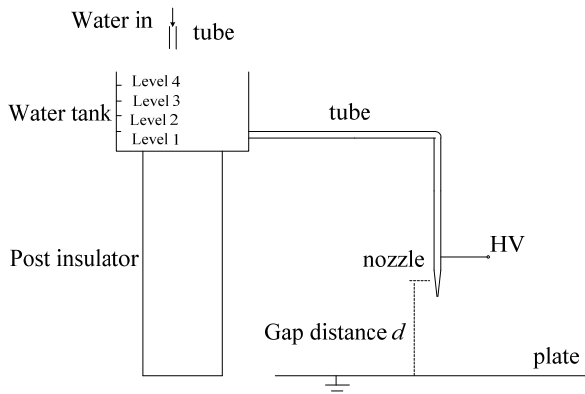


Figure 5. Experiment set up.

The experimental set up is illustrated in Figure 5. Water was stored in a tank to maintain constant pressure. Conductivities of $80 \mu\text{S}/\text{cm}$ to $1000 \mu\text{S}/\text{cm}$ – which reflect the range of very clean rain in Manchester and polluted rain of $700 \mu\text{S}/\text{cm}$ in Beijing. Since flashover may be affected by initial pollution on sheds, a higher top value of $1000 \mu\text{S}/\text{cm}$ was also used. The nozzle was fed by a copper tube of 11.9 mm internal diameter, D_1 , and had the HV line directly attached. The water tank of length 40 cm , width 30 cm , and height 40 cm was supported by post insulator with a height of 100 cm . The tap water was directed vertically downward through the nozzle into still air with speed v , which is determined by dividing the flow rate Q by $\pi(D_1/2)^2$, and controlled by adjusting the water level in the tank. To keep the water level constant, an insulated tube connected to a pump system was used as the water supply. In this paper, four different water levels were used. In our tests, the velocity of the water stream is always smaller than the critical velocity v_{c2} which distinguishes the Rayleigh regime and first break-up regime (Figures 2 and 3).

The ac voltage was generated by an $800 \text{ kV} / 0.5 \text{ A}$ transformer and measured to within 2% . In all of the experiments a uniform increase in voltage of 5 kV/s was used. At least 10 experiments were performed for each condition.

This investigation relates to extreme, very short term weather events (of the order of minutes) which generate high rainfall levels over a short period of time. Direct measurements of this with good spatial resolution are not currently available. In [18], it gives 6 min averages of $2.5 \text{ mm}/\text{min}$ as extreme, which supports the description of $1 \text{ mm}/\text{min}$ by the UK Metrological Office as ‘a violent rain shower’. A vertical $2.5 \text{ mm}/\text{min}$ deposits $2125 \text{ mm}^3/\text{s}$ on the top surface of a 255 mm diameter insulator. If this accumulation runs off the insulator in one place with a flow diameter of 2 mm we would see a

flow rate of 0.7 m/s . If the rain was inclined to the axis of the insulator the effective capture area would effectively increase giving higher flow rates. A 4 m long insulator with a 30° inclination to the rain gives a potential capture of $21,200 \text{ mm}^3/\text{s}$. Given half of this creates a single flow, a stream of 1.5 m/s results. These issues are worthy of more research, but lead to the choice of water flow rates of between 0.7 and 2 m/s , and are consistent with laboratory experience [19].

3 TEST RESULTS

The ac breakdown voltages of four different rod-plane air gap separations (23.0 , 30.0 , 34.0 and 40.5 cm) were investigated under different conditions. Test results are given in Figure 6 - Figure 9, in which d is the gap separation, cm ; v is the average velocity of water stream, m/s ; D is the inside diameter of nozzle, mm ; U_b is the ac breakdown voltage, kV ; δ is the standard deviation, kV .

3.1 COMPARISON BETWEEN DRY AND WATER STREAM CONDITIONS

Figure 6 shows the relationship between the breakdown voltage U_b and gap separation d when the diameter of nozzle D is 3 mm and the average velocity of water stream v is 0.75 and 1.02 m/s respectively. Results from dry conditions in which the ambient temperature T was 18°C and the relative humidity RH was 53% are also given.

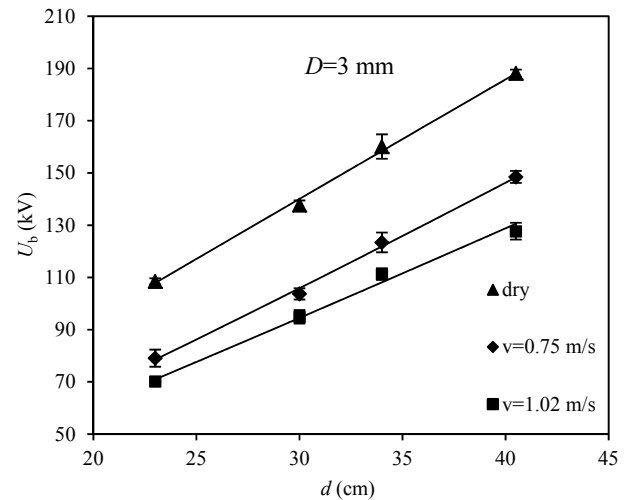


Figure 6. Breakdown voltage variation with gap distance.

As shown in Figure 6, the presence of the water stream decreases the breakdown voltage of rod-plane air gap. The relative variation of breakdown voltage corresponding to Figure 6 can be seen in Table 1, where the breakdown voltage in dry conditions is regarded as the reference value. It can be seen that the average reduction of breakdown voltage is 24% (with a 3% standard deviation) and 29% (with a 5% standard deviation) when $v = 0.75 \text{ m/s}$ and 1.02 m/s respectively. The reduction of breakdown voltage appears to increase with the increase of the water stream velocity. Further test results concerning this will be presented in section 3.2. According to Table 1, the effect of water stream on the breakdown voltage is

likely to get smaller with an increase of the gap separation.

Table 1. Relative variation of breakdown voltage with different water stream velocity.

$d(\text{cm})$	$v = 0.75 \text{ m/s}$	$v = 1.02 \text{ m/s}$
	α (%)	β (%)
23.0	-27.1	-35.3
30.0	-24.7	-31.1
34.0	-22.9	-24.3
40.5	-21.1	-27.1

By fitting the test results in Figure 6 with the least squares method, the mathematical relationship between breakdown voltage and gap separation can be obtained as follows:

$$U = \begin{cases} 4.6d + 1.8 & \text{dry} \\ 4.0d - 14.2 & v = 0.75 \text{ m/s} \\ 3.3d - 5.2 & v = 1.02 \text{ m/s} \end{cases} \quad (4)$$

where, the coefficient R^2 for each case is 0.9975, 0.9967 and 0.9911.

3.2 INFLUENCE OF WATER STREAM VELOCITY

To investigate further the influence of the velocity of the water stream on the breakdown voltage, another group tests are presented in Figure 7.

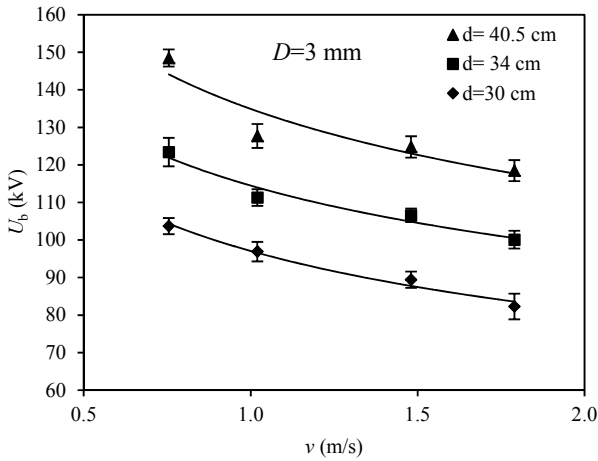


Figure 7. Breakdown voltage variation with water stream velocity.

From Figure 7, it can be seen that the breakdown voltage of the rod-plane air gaps of 30, 34 and 40.5 cm decreases with an increase of water stream velocity. When the velocity is 1.79 m/s, the breakdown voltages for the gap distance of 40.5, 34 and 30 cm have the lowest values of 118.5, 100.1 and 82.3 kV respectively, and the corresponding reductions relative to the dry conditions are 37%, 38% and 40%. The lines of best fit in Figure 7 show the relationships.

$$U = \begin{cases} 134.9v^{-0.235} & d = 40.5 \text{ cm} \\ 114.5v^{-0.224} & d = 34 \text{ cm} \\ 97.1v^{-0.257} & d = 30 \text{ cm} \end{cases} \quad (5)$$

where, the coefficient R^2 for each case is 0.8702, 0.9575 and 0.9791.

3.3 INFLUENCE OF NOZZLE DIAMETER

Figure 8 shows variation of breakdown voltage on internal nozzle diameter, D . It can be seen that the breakdown voltage decreases with an increase of the nozzle diameter. The relative reduction of breakdown voltage, taking the value at $D=1 \text{ mm}$ as the reference is given in Table 2.

The test results of Figure 8, have been fitted to a linear function with resulting correlation coefficients, R^2 , of 0.9813, 0.9504 and 0.9329.

$$U = \begin{cases} -6.4D + 123.1 & v = 0.75 \text{ m/s} \\ -9.4D + 124.9 & v = 1.0 \text{ m/s} \\ -9.8D + 120.6 & v = 1.48 \text{ m/s} \end{cases} \quad (6)$$

From equations (6), we can see that the average relative breakdown voltage $\zeta(D)$ will decrease with an increase of nozzle diameter by 2.9% / 0.5 mm, 4.3% / 0.5 mm and 4.76% / 0.5 mm for the water stream velocity of 0.75 m/s, 1.0 m/s and 1.48 m/s respectively.

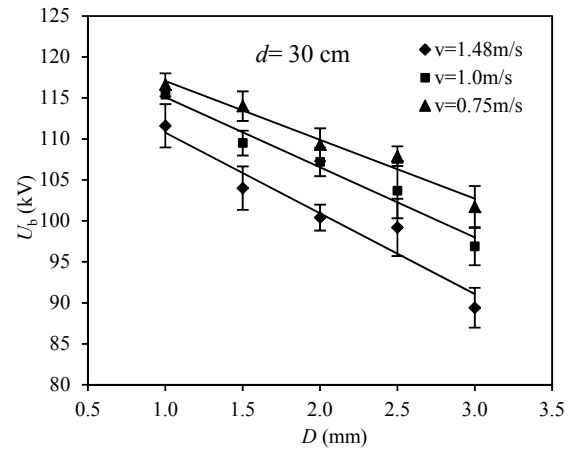


Figure 8. Breakdown voltage variation with internal nozzle diameter.

Table 2. Relative reduction of breakdown voltage with nozzle diameter.

$D(\text{mm})$	$v = 0.75 \text{ m/s}$	$v = 1.02 \text{ m/s}$	$v = 1.48 \text{ m/s}$
	α (%)	β (%)	σ (%)
1.5	-2.2	-5.1	-6.8
2.0	-6.3	-7.1	-10.0
2.5	-7.5	-10.1	-11.1
3.0	-11.1	-17.8	-19.9

3.4 INFLUENCE OF WATER CONDUCTIVITY

In addition to the water stream velocity and nozzle diameter, the effect of water conductivity on the breakdown voltage of the air gap has been investigated. Conductivity was increased by adding a controlled amount of NaCl to the water supply. The test results and conditions are given in Figure 9. Table 3 indicates the relative variation of U_b when the water conductivity increases from 80 to 1000 $\mu\text{S/cm}$, where $\Delta U = 100\% \times (U_{b1000} - U_{b80}) / U_{b80}$, and U_{b1000} , U_{b80} are the breakdown voltage corresponding to $\gamma_{20} = 1000 \mu\text{S/cm}$ and $80 \mu\text{S/cm}$, respectively. The breakdown voltage of the air gap decreases as the water conductivity increases.

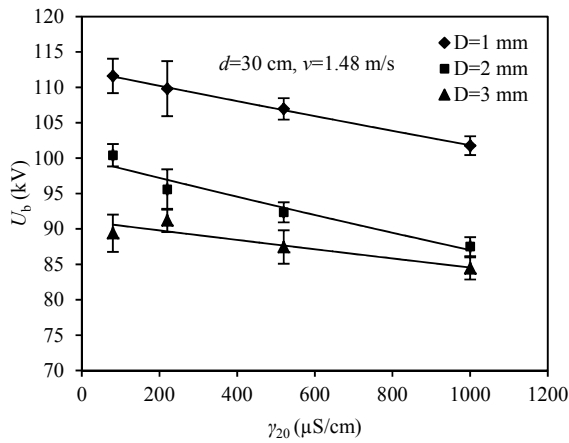


Figure 9. Breakdown voltage variation with water conductivity.

Table 3. Relative reduction of breakdown voltage with water conductivity.

D (mm)	γ_{20} ($\mu\text{S/cm}$)	U_b (kV)	ΔU (%)
1.0	80	111.6	-8.8
	1000	101.8	
2.0	80	100.4	-12.8
	1000	87.5	
3.0	80	89.4	-5.6
	1000	84.4	

4 VISUAL OBSERVATIONS

To investigate the effect of the electrical field on the break-up length of the water stream, a high speed camera was used to take the photographs of the water stream in various conditions. For each case, 600 consecutive images at a frame rate of 1000 fps and 768×768 pixel spatial resolution were recorded with an exposure time of $820 \mu\text{s}$.

Some typical images are shown in Figure 10. It is clear that increasing the applied voltage decreases the break-up length of water stream. Moreover, as the electrical field increases, a stronger waving motion at the tip of the water stream occurs, making the formed droplets fall away from the vertical axis. It can also be seen that the water stream does not flow smoothly. Its surface behaves like a wave with a certain wavelength (see also Figure 1). However, such wave-like phenomena appear to

be less obvious as the applied voltage is increased.

Regarding the water droplets, it can be seen that increasing the electrical field reduces the droplets in size, increases their number and leads to a greater spatial distribution away from the vertical axis. The droplet volume at pinch-off (on separation from the jet) can be determined by the assumption [12], [20] that the droplet's mass is equal to that of a cylinder one wavelength long. Thus, according to Son and Ohba's theory [12], that the wavelength decreases with the increase of electrical field strength, it can be explained that the increasing of the electrical field reduces the size of the separated droplet.

Additionally, it can also be observed that there are air-borne or satellite droplets around the main droplets and similarly, the number of satellite droplets increases with the electrical field strength. According to [21], the formation of satellite droplets is due to a ligament between the main droplets after break-up, which gradually becomes spherical and forms the satellite drop.

4.1 EFFECT OF ELECTRICAL FIELD ON THE CRITICAL BREAK-UP LENGTH AND DROPLET SIZE

To further investigate the characteristics of a water stream under conditions of different velocity, internal nozzle diameter and applied voltage, the critical break-up length and main droplets size were measured using image process software. The results are shown in Figure 11 and Figure 12, where L_b is the average critical break-up length of a water stream, mm; D_w is the average diameter of main droplets, mm; U_0 is the applied voltage, kV.

In accordance with the generalised observations in Figure 10, it can be seen from Figure 11 and Figure 12 that L_b and D_w both decrease as applied voltage increases. However, after the applied voltage rises above a certain value, the rate of decrease of L_b and D_w becomes small and appears to tends to a constant value. That is to say, quasi minimum values of L_b and D_w are reached.

From Figure 11, it may be seen that the effect of the applied voltage on the critical break-up length of a water stream is similar in nature independent of jet velocity, but its influence is greater on the larger diameter streams. Similar observations may be made on the water droplet size. These observations are consistent with the test results carried out by *Garmendia* and *Smith* [22].

In accordance with the generalised observations in Figure 10, it can be seen from Figure 11 and Figure 12 that L_b and D_w both decrease as applied voltage increases. However, after the applied voltage rises above a certain value, the rate of decrease of L_b and D_w becomes small and appears to tends to a constant value. That is to say, quasi minimum values of L_b and D_w are reached.

From Figure 11, it may be seen that the effect of the applied voltage on the critical break-up length of a water stream is similar in nature independent of jet velocity, but its influence is greater on the larger diameter streams. Similar observations may be made on the water droplet size. These observations are consistent with the test results carried out by *Garmendia* and *Smith* [22].

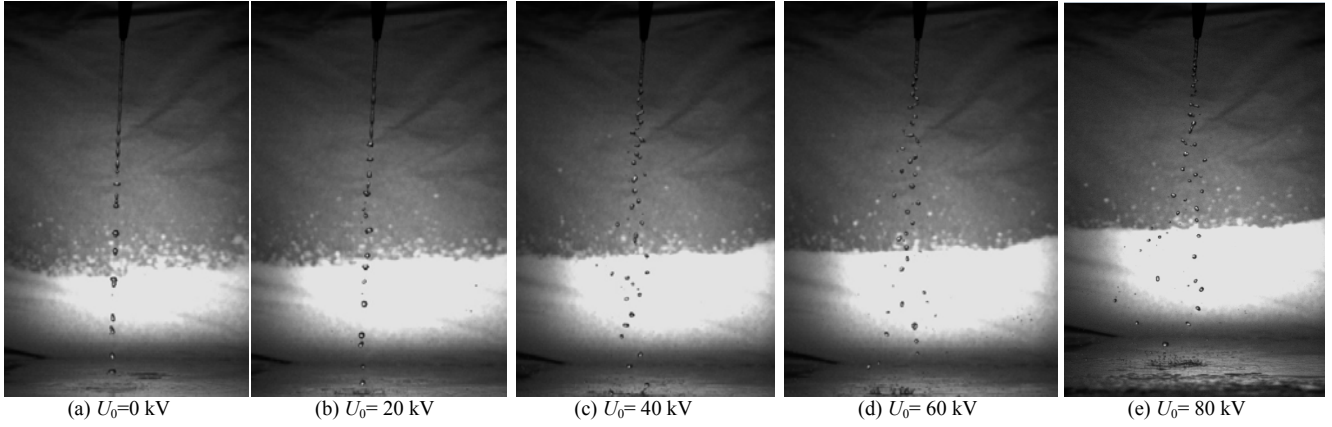


Figure 10. Break-up length of water stream under different applied voltage ($D=3$ mm, $v=1.0$ m/s, $d=30$ cm).

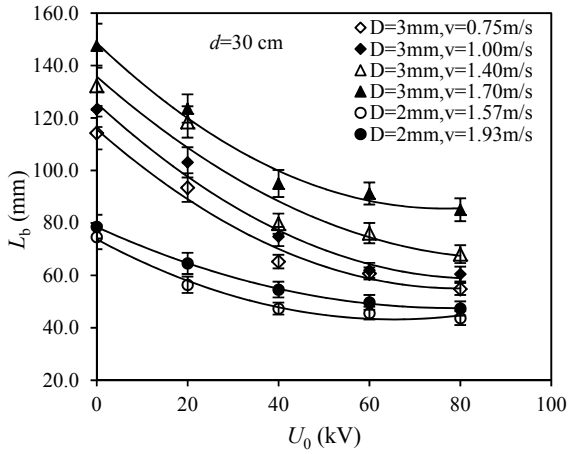


Figure 11. Relationship between critical break-up length and applied voltage.

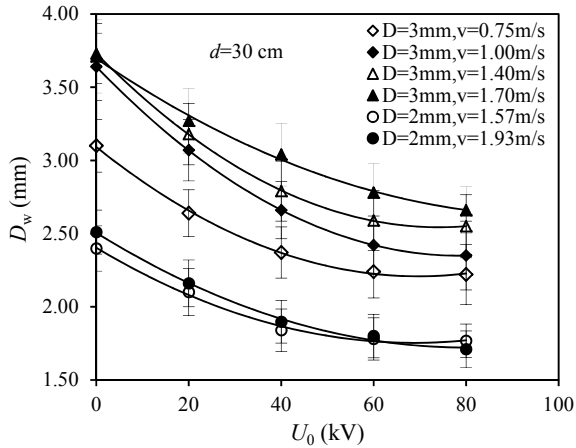


Figure 12. Relationship between droplet diameter and applied voltage.

The results in Figure 11 and Figure 12 were fitted to an exponential function. The best fits are given in equations (7) and (8) respectively. According to equation (7), the average value of index coefficients of L_b at different jet velocities are

about -0.009 and -0.006 for the $D=3$ mm and $D=2$ mm respectively. The average value of index coefficients of D_w in all studied cases is -0.0046 .

$$L_b = \begin{cases} 140.6e^{-0.007U_0} & D=3\text{mm}, v=1.70\text{m/s} & R^2=0.92 \\ 130.6e^{-0.009U_0} & D=3\text{mm}, v=1.40\text{m/s} & R^2=0.91 \\ 119.8e^{-0.01U_0} & D=3\text{mm}, v=1.00\text{m/s} & R^2=0.94 \\ 109.2e^{-0.01U_0} & D=3\text{mm}, v=0.75\text{m/s} & R^2=0.93 \\ 67.8e^{-0.006U_0} & D=2\text{mm}, v=1.57\text{m/s} & R^2=0.85 \\ 74.7e^{-0.006U_0} & D=2\text{mm}, v=1.93\text{m/s} & R^2=0.94 \end{cases} \quad (7)$$

$$D_w = \begin{cases} 3.62e^{-0.004U_0} & D=3\text{mm}, v=1.70\text{m/s} & R^2=0.97 \\ 3.56e^{-0.005U_0} & D=3\text{mm}, v=1.40\text{m/s} & R^2=0.92 \\ 3.49e^{-0.006U_0} & D=3\text{mm}, v=1.00\text{m/s} & R^2=0.94 \\ 2.95e^{-0.004U_0} & D=3\text{mm}, v=0.75\text{m/s} & R^2=0.89 \\ 2.29e^{-0.004U_0} & D=2\text{mm}, v=1.57\text{m/s} & R^2=0.87 \\ 2.41e^{-0.005U_0} & D=2\text{mm}, v=1.93\text{m/s} & R^2=0.94 \end{cases} \quad (8)$$

4.2 BREAKDOWN PROCESS

The moment when the breakdown of the air gap in the presence of the water stream occurs has been captured using a high speed camera. The recorded images are shown in Figure 13. It can be observed that the spark, originating from the nozzle electrode, progresses along the water stream surface, and then traverses the remaining air gap. Additionally, from Figure 13b, 13e and 13f, it is evident that the spark passes over the surface of the water droplets. But for most cases, the spark is likely to develop in free air.

Generally, when there are droplets in the air gap, the electric field can be significantly distorted: the field inside the droplet is relatively lower and the field around the surface of the droplet increases. To account for this augmentation of the local field around the droplet, several FEA simulations have been carried out with different droplet sizes and separations, as

illustrated in Figure 14. Without droplets it can be seen that the field distribution from plane to rod is very smooth as there are no discontinuities in the air gap, and the maximum field located at the tip of rod is about 22.5 kV/cm. However, water droplets affect the field distribution in the air gap significantly. Moreover, it can also be observed that the field distortion resulting from droplets which are close to the rod is more intense than that caused by droplets near the plane. That is to say, the effect exerted by the water droplets is determined by the distance from the droplet to the water source.

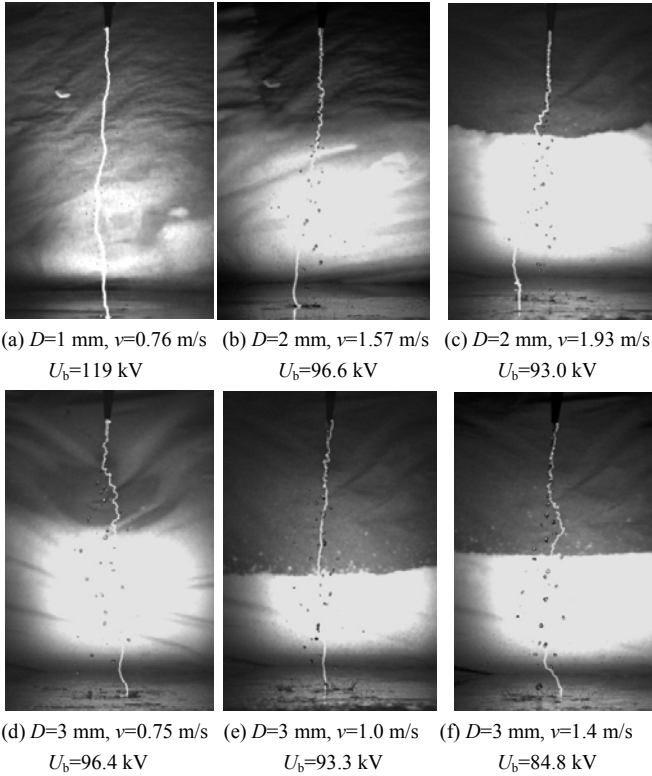


Figure 13. Breakdown images of rod-plane air gap in the presence of a water stream ($d=30$ cm, $\gamma_{20}=80$ $\mu\text{S/cm}$).

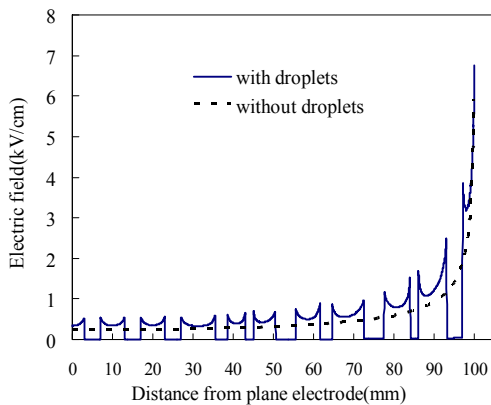


Figure 14. Field intensity curve of rod-plane air gap with and without rain drops of different sizes and separations.

4.3 COMPARISON OF DROPLETS SIZE FROM TEST RESULTS AND THE THEORETICAL MODEL

By solving the maximum value of growth rate ω_{\max} in equation (3), the critical wavelength that is used to calculate the radius of droplet can be obtained with the following equations proposed in [23]:

$$D_w^* = (12\pi)^{1/3} \left(\frac{\lambda_{cr}}{\pi D} \right)_{\max \omega}^{1/3} (D/2) \quad (9)$$

Where D_w^* is the diameter of the water droplet.

Thus, combining equation (3) and (9), D_w^* can be obtained at different voltage levels. The difference between the experimental and theoretical results can be seen in Figure 15.

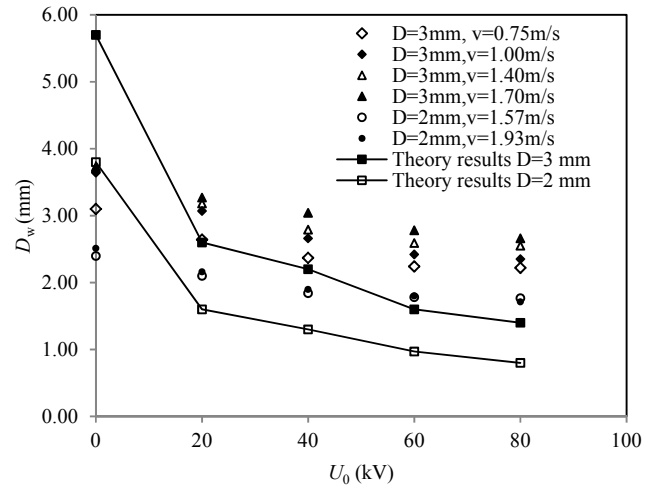


Figure 15. Comparison of droplets size between test results and the theoretical model.

For the theoretical model, the calculated droplet diameter in the cases of $D=3$ mm and $D=2$ mm without applied voltage is greater than the experimental values. However, the calculated droplet diameter decreases much faster than that obtained from the experiments as the voltage is applied.

The reason for the disagreements between the theoretical and experimental results may result because the effects of the velocity of the water stream and the surrounding air on the development of the stream wave are neglected in this model.

5 DISCUSSION

5.1 FACTORS INFLUENCING THE BREAK-UP OF A WATER STRAEM

The break-up length of a water stream or water jet is determined by such factors as air streams [22], electric field [12]-[20], liquid velocity [24]-[25], nozzle size [28] and so on. Also, as shown in Figure 6, the breakdown voltage of a rod-plane air gap is decreased by the presence of a water stream. The reason for that is principally that the water stream shortens the air gap. According to Figure 7 and Figure 8, the breakdown voltage of the air gap varies with the velocity and the initial diameter of water stream. Therefore these two parameters are discussed in the following sections.

5.1.1 EFFECT OF WATER STREAM VELOCITY

As stated previously, by virtue of surface tension, the Plateau-Rayleigh instability jet tends to minimize its surface area, resulting in the break-up of the water stream and the formation of droplets. However, the velocity of the water stream can play an essential role in the break-up process. Firstly, when the velocity of the water stream is very small, that is to say the kinetic energy is much smaller than the surface energy, it will break-up at an extremely small length, instinctively we know this as “dripping”. But, when the water flow rate is progressively increased such that the water stream velocity is relatively large so that the kinetic energy overcomes the surface energy, a continuous water stream will be formed.

In [30], *Lin* and *Reitz* pointed out that the criterion for Plateau-Rayleigh jet break-up could be expressed in terms of the Weber number:

$$We_L > 8 \quad \text{and} \quad We_g = \frac{\rho_g}{\rho_L} We_L < 0.4 \quad (10)$$

where ρ_g is the air density, kg/m³. The Weber number for a fluid in equation (5), $We_L > 8$ is the criterion that dripping can no longer occur from the nozzle exit or the jet could be formed, and $We_g < 0.4$ corresponds to the point where the inertial force of the surrounding gas can be ignored in comparison with the surface tension force.

When the water stream velocity is further increased, the surrounding gas accelerates the break-up process, shortening the break-up length of water stream [31]. As a result, the break-up length of Plateau-Rayleigh jet is proportional to the jet velocity as long as the Weber number of liquid and the surrounding gas meet the conditions of inequalities (10) [30]. According to the calculated Weber numbers in this paper, the water streams formed in our tests are all within the Plateau-Rayleigh break-up regime and the effect of the air stream can be neglected. Thus, the increase of water stream velocity can lead to a longer continuous filament of water in the gap, effectively reducing the breakdown distance and thus decreasing of breakdown voltage of air gap.

5.1.2 EFFECT OF NOZZLE DIAMETER

In addition to the water jet velocity, the initial diameter of water stream or the nozzle diameter also affects the break-up length of water stream and the breakdown voltage of the air gap.

According to [10], *Rayleigh* showed that a vertically falling water stream with a circular cross section should break up into drops if its wavelength exceeded its circumference, or π times its diameter, D . Later, considering the wavelength of a water jet, λ , Weber [32] extended Rayleigh’s instability research and gave the λ_{\min} and λ_{opt} , as

$$\lambda_{\min} = \pi D, \quad \lambda_{\text{opt}} = \sqrt{2\pi D(1 + 3Oh)^{0.5}} \quad (11)$$

Where $Oh = \mu_L / (D\sigma\rho_L)^{0.5}$ is the Ohnesorge number, and μ_L is the dynamic viscosity of water [33]. When the wavelength is greater than λ_{\min} , disintegration will occur due to the effect of surface tension force. But in the case that the wavelength is smaller than λ_{\min} , the surface force will not result in the break-up. The wavelength of λ_{opt} is the most favorable length for break-up and droplet formation. Additionally, in [34], Sallam

summarized measurements of the critical break-up length of liquid jets and obtained the best-fit correlation for the weakly turbulent break-up length (Rayleigh break-up) as:

$$L_b = 5.0D\sqrt{We} \quad (12)$$

Thus, through equations (11) and (12), it can be determined that the wavelength of the Rayleigh jet is related to its initial diameter, and with the increase of this value, the minimum wavelength of the water jet will increase, eventually leading to the increase of the break-up length of a water stream.

On the other hand, it is believed that the larger the diameter of the nozzle is, the less will be the effect of the applied voltage on the water stream. In other words, a water stream with larger initial diameter is more difficult to break-up under the same voltage level and thus has a longer break-up length. To account for this point, we measured the average break-up time interval Δt with an applied voltage of 80 kV. In each case, hundreds of images are used to improve the accuracy of the measurement.

Table 4. Measured results of Δt .

$D(\text{mm})$	$v(\text{m/s})$	$\Delta t(\text{ms})$	$\Delta t_{\text{ave}}(\text{ms})$
3.0	0.75	7.1	7.1
	1.00	7.4	
	1.40	6.7	
	1.70	7.1	
2.0	1.57	5.8	5.7
	1.93	5.6	

Note: the applied voltage is 80 kV for all the results above.

It can be observed that Δt for a fixed diameter of water stream appears to be independent of the velocity, v , of the water stream. Thus, it can be said that the average break-up time interval is only determined by the diameter of the water stream. Additionally, the break-up time interval of $D = 3$ mm is 7.1 ms, larger than the one of $D = 2$ mm, which means the break-up length of a water stream with a larger diameter is longer than the smaller one as the velocity is the same.

In addition to affecting the break-up length of a water stream, the nozzle diameter can also influence the size of water droplets formed after the break-up, as shown in section 4.1. As analyzed in [35], the formation of water droplets in the air gap distorts the electrical field significantly on the one hand, and on the other hand, water droplets could be regarded as electron sources and emit ions due to their relative low ionization energy, supplying the stream head and promoting avalanches. Moreover, with the increase of the radius and number of droplets, the maximum electric field in the air gap will also increase. That is to say, the formation of water droplets will reduce further the breakdown voltage of the air gap.

Thus, the increase of nozzle diameter will affect the breakdown voltage of air gap in two ways: firstly by increasing the break-up length of water jet and shortening the effective air gap length, and secondly by increasing the radius of water droplets within the remaining gap and further distorting and enhancing the electric field in that region.

5.2 PREVENTION MEASURES

According to our test results, the reduction of breakdown voltage is related to the water stream velocity, diameter and conductivity. In practice, the nature of any water column formed at the HV end of an insulator string is unlikely to be

known, including its length. However, based on our experimental results, the maximum decrease of breakdown voltage is by 40% for a gap of 40 cm. This provides a reference for the insulation clearance design of low voltage levels, for example on 10 kV and 35 kV systems in rainstorm areas. As for higher voltage systems, further tests would be desirable for long air gaps.

According to our test results, the formation of a water stream can decrease the electrical strength of overhead line insulation significantly. Thus, the key to preventing breakdown accidents from heavy rain is to reduce the possibility of the formation of a water stream. Therefore, several mitigation measures may be considered in areas prone to heavy rainfall: (1) Change vertical suspension insulator strings for horizontal strings or “V” strings. (2) For normal suspension ceramic or glass insulator strings which cannot be changed into horizontal or “V” strings, use insulators with large diameters instead. (3) Coat the insulators with RTV or PRTV to prevent the formation of water films on their surfaces.

6 CONCLUSIONS

The presence of a water stream reduces the ac breakdown voltage of a rod-plane air gap significantly in comparison with dry conditions (up to 40%). The ac breakdown voltage of such an air gap is decreased by an increase of water stream velocity, diameter and conductivity. For the case of water conductivity increasing from 80 to 1000 $\mu\text{S}/\text{cm}$, the relative breakdown voltage for nozzle diameters of 1.0, 2.0 and 3.0 mm is -8.78%, -12.84% and -5.59%. These changes less than those measured due to the water stream velocity and diameter since it is the physical length of the protruding stream and the size of the water droplets in the remaining air gap which dominate the breakdown characteristics. In the higher flow case, increasing the nozzle diameter from 1 mm to 3 mm decreased the breakdown voltage by 20% because a broader stream with high velocity tends to longer stream breakup lengths, thereby reducing breakdown voltages.

With the increase of the applied voltage, the critical break-up length and the size of main water droplets tend to be decreased. The effect of the electrical field and water conductivity on the break-up length of a water stream and the size of droplets is similar for all the jet velocities studied. Further work is required on the relationship between these parameters.

The parameters used of this work are based on laboratory experience and limited weather data sets. More work is required to both determine insulators' behavior in short-term extreme precipitation conditions, and to understand the likelihood of such conditions occurring. Only then can the likelihood of flashover caused by water streams in natural conditions be quantified.

ACKNOWLEDGMENT

This work is supported by National Basic Research Program of China (Grant NO. 2009CB724501/502) and National Natural Science Foundation of China (Grant NO. 51107151).

REFERENCES

- [1] Y. Hu, “Analysis on operation faults of transmission line and counter measures”, *High Voltage Engineering*, Vol. 33, No.3, pp. 1-8, 2007 (in Chinese).
- [2] F. A. M. Rizk. “Electrical resistance of an insulating surface under artificial rain”, *Proc IEE*, Vol. 121, pp. 154-160, 1974.
- [3] F. A. M. Rizk, “Influence of Rain on Switching impulse sparkover voltage of large-electrode air gaps”, *IEEE Trans. Power App. Syst.*, Vol. 95, pp. 1394-1402, 1976.
- [4] Y. Yamagata, A. Oe, K. Miyake, Y. Aihara and T. Shindo, “Phase-to-ground and phase-to-phase sparkover characteristics of external insulation at the entrance of a UHV substation”, *IEEE Trans. Power Delivery*, Vol. 17, pp. 223-232, 2002.
- [5] Y. Hu, L. N. Wang, G. W. Shao, K. Liu, C. L. Luo, S. J. Chen and C. Y. Geng, “Influence of rain and wind on power frequency discharge characteristic of conductor-to-tower air gap”, *High Voltage Engineering*, Vol. 34, No. 5, pp. 845-850, 2008 (in Chinese).
- [6] Y. Yuan, X. L. Jiang, Y. Du, J. G. Ma and C. X. Sun, “Predictions of the AC discharge voltage of short rod-plane air gap under rain conditions with the application of ANN”, *High Voltage Engineering*, Vol. 38, No. 1, pp. 102-108, 2012 (in Chinese).
- [7] X. L. Jiang, S. J. Xi, W. Liu, Y. Yuan, Y. Du and J. G. Ma, “Influence of rain on AC discharge characteristic of rod-plane (rod-rod) air gap”, *Journal of Chongqing University*, Vol. 35, No. 1, pp. 52-58, 2012 (in Chinese).
- [8] A. Tzimas, S. M. Rowland and J. Barrett. “The influence of surface ageing features of insulators on wet flashover performance”, *IEEE Conf. Electr. Insul. Dielectr. Phenomena*, 2010.
- [9] J. Plateau. “Experimental and theoretical researches on the figures of equilibrium of a liquid mass withdraw from the action of gravity”, *Annual Report of the Board of Regents of the Smithsonian Institution*, pp. 270-283, 1863.
- [10] L. Rayleigh. “On the instability of jets”, *Proc. Lond. Math. Soc.*, Vol. 10, No. 1, pp. 4-13, 1879.
- [11] L. Rayleigh. “On the instability of a cylinder of viscous liquid under the capillary force”, *Phil. Mag.*, Vol. 34, Issue. 207, pp. 145-154, 1892.
- [12] P. H. Son and K. Ohba. “Theoretical and experimental investigations on instability of an electrically charged liquid jet”, *Int'l. J. Multiphase Flow*, Vol. 24, No. 4, pp. 605-615, 1998.
- [13] O. Breslouer. “Rayleigh-plateau instability falling jet”, *Project Report*, Princeton University. 2010.
- [14] J. Delteil, S. Vincent, A. Erriguible and P. S. Paternault. “Numerical investigations in rayleigh breakup of round liquid jets with VOF methods. *Computer Fluids*”, Vol. 50, No. 1, pp. 10-23, 2011.
- [15] J. B. Blaisot and S. Adeline. “Determination of the growth rate of instability of low velocity free falling jets”, *Experiments in Fluids*, Vol. 29, No. 3, pp. 247-256, 2000.
- [16] A. M. Sterling and C. A. Sleicher. “The instability of capillary jets”. *J. Fluid. Mech.*, Vol. 68, No. 3, pp. 477-495, 1975.
- [17] M. Szakáll, S. K. Mitra, K. Diehl and S. Borrmann. “Shapes and oscillations of falling raindrops - A review”, *Atmospheric Research*, Vol. 97, No. 4, pp. 416-425, 2010.
- [18] A. Berne, G. Delrieu, J. D. Creutin and C. Obled. ‘Temporal and spatial resolution of rainfall measurements required for urban hydrology’, *J. Hydrology*, Vol. 299, pp 166-179, 2004.
- [19] A. Tzimas and S. M. Rowland, “Asymmetrical ageing of composite insulators: effect on water dripping behavior and electrical performance”, *IEEE Int'l. Sympos. Electr. Insul. (ISEI)*, pp. 1-5, 2010.
- [20] R. T. Collins, M. T. Harris and O. A. Basaran. “Breakup of electrified jets”, *J. Fluid. Mech.*, Vol. 588, pp. 75-129, 2007.
- [21] N. Ashgriz and F. Mashayek. “Temporal analysis of capillary jet breakup”, *J. Fluid Mech.*, Vol. 291, pp. 163-190, 1995.
- [22] L. A. Garmendia and I. K. Smith, “The effects of an electrostatic field and air stream on water jet break-up length”, *Canadian J. Chemical Eng.*, Vol. 53, No. 6, pp. 606-610, 1975.
- [23] A. L. Huebner and H. N. Chu. “Instability and breakup of charged liquid jets”, *J. Fluid Mech.*, Vol. 49, No. 2, pp. 361-372, 1971.
- [24] W. Debler and D. Yu. “The break-up of laminar liquid jets”, *Proc. R. Soc. Lond.*, Vol. 415, No. 1848, pp. 107-119, 1988.
- [25] R. P. Grant and S. Middleman. “Newtonian jet stability”, *American Institute of Chemical Engineers*, Vol. 12, Issue 4, pp. 669-678, 1966.
- [26] E. F. Goedde and M. C. Yuen, “Experiments on liquid jet instability”, *J. Fluid Mech.*, Vol. 40, No. 3, pp. 495-511, 1970.

- [27] M. Goldin, J. Yerushalmi, R. Pfeffer and R. Shinnar. "Breakup of a laminar capillary jet of a viscoelastic fluid", *J. Fluid Mech.*, Vol. 38, No. 4, pp. 689-711, 1969.
- [28] A. Umemura, S. Kawanabe, S. Suzuki and J. Osaka. "Two-valued breakup length of a water jet issuing from a finite-length nozzle under normal gravity", *Amer. Phys. Soc.*, Vol. 84, No. 3, pp. 036309(1-22), 2011.
- [29] S. S. Dukhin, C. Zhu, R. Dave, R. Pfeffer, J. J. Luo, F. Chávez, Y. Shen. "Dynamic interfacial tension near critical point of a solvent-antisolvent mixture and laminar jet stabilization". *Colloids and Surfaces A: Physicochem. Eng.*, Vol. 229, No. 1-3, pp. 181-199, 2003.
- [30] S. P. Lin and R. D. Reitz. "Drop and spray formation from a liquid jet", *Annual Review of Fluid Mechanics*, Vol. 30, pp. 85-105, 1998.
- [31] W. V. Hoeve, S. Gekle, J. H. Snoeijer, M. Versluis, M. P. Brenner and D. Lohse. "Breakup of diminutive rayleigh jets", *Phys. Fluids*, Vol. 22, No. 12, pp. 122003(1-11), 2010.
- [32] C. Z. Weber, "Zum zerfall eines flüssigkeitsstrahles", *Z. Angew. Math. Mech.*, Vol. 11, pp. 136-154, 1931. (In German).
- [33] Y. Pan and K. Suga, "A numerical study on the breakup process of laminar liquid jets into a gas", *Phys. Fluids*, Vol. 18, No. 5, pp. 1-11, 2006.
- [34] K. A. Sallam, Z. Dai and G. M. Faeth, "Liquid breakup at the surface of turbulent round liquid jets in still gases", *Int'l. J. Multiphase Flow*, Vol. 28, No. 3, pp. 427-449, 2002.
- [35] X. L. Jiang, Y. Yuan, M. Q. Bi, Y. Du and J. G. Ma. "DC positive discharge performance of rod-plane short air gap under rain conditions", *IEEE. Trans. Dielectr. Electr. Insul.*, Vol. 20, No. 1, pp. 104-111, 2013.



Yao Yuan was born in Sichuan, China, in 1987. He received the B.Sc. degree from Chongqing University, China in 2009. He is currently pursuing the Ph.D. degree in the college of electrical Engineering, Chongqing University. He is mainly engaged in the field of high-voltage external insulation and discharge performance and mechanism of air gap. He is currently studying in the School of Electrical and Electronic Engineering in Manchester University as an exchange student.



Xingliang Jiang was born in Hunan province, China, in 1961. He graduated from Hunan University in 1982 and got his M. Sc. degree and Ph. D. degree in Chongqing University in 1988 and 1997, respectively. He published his first monograph—Transmission Line's Icing and Protection in 2001, and has published over 100 papers about his professional work. He received the Second-class Reward for Science and Technology Advancement from Ministry of Power in 1995, Beijing Government in 1998, Ministry of Education in 1991 and 2001, respectively, the First-class Reward for Science and Technology Advancement from Ministry of Power in 2004, the Third-class Reward for Science and Technology Advancement from Ministry of Power in 2005, the Second-class Reward for Science and Technology Advancement from Ministry of Technology in 2005 and 2009, the First class Reward for Science and Technology Advancement from Ministry of Education in 2007, and the First-class Reward for Science and Technology Advancement from Chongqing Government in 2007.



Simon M. Rowland (SM'07-F'14) was born in London, England. He completed the B.Sc. degree in physics at The University of East Anglia and the Ph.D. degree at London University. He was awarded the IEE Duddell Premium in 1994 and became a FIEE in 2000. He has worked for many years on dielectrics and their applications and has also been Operations and Technical Director within multinational manufacturing companies. He joined The School of Electrical and Electronic Engineering in The University of Manchester as a Senior Lecturer in 2003, and was

appointed Professor of Electrical Materials in 2009. He was appointed the President of the IEEE Dielectric and Electrical Insulation Society from 2011 – 2012.



Xian Cheng was born in Henan province, China, in November, 1982. He received the B.S. degree from Air Force Engineering University, Xi'an, China, in 2003, the M.S. degrees from the Huazhong University of Science and Technology, Wuhan, China, in 2007 and the Ph.D degrees from the Dalian University of Technology, Dalian, China, in 2012. He is currently a Research Associate in the School of Electrical and Electronic Engineering, the University of Manchester. He is presently engaged in the study of high voltage technology, especially in

the field of Low-carbon Intelligent Circuit Breaker and Electric Shock Peening Technology.



Qi Li (aka Steven) was born in Hunan Province, China, in September 1984. He completed the B.Eng. degree in Electrical and Electronics Engineering at both the University of Birmingham and Huazhong University of Science and Technology, in 2007 (as an exchange student). He received the M.Sc. degree with distinction in electrical power engineering from the University of Manchester in 2009, and completed the Ph.D. degree in the same institution in 2014. Dr Qi Li is currently working as a research assistant in the National Grid High Voltage Research

Centre in the University of Manchester, UK. His main research interests include: surface potential gradient calculation for overhead line conductors, the mechanism of hum noise from transmission lines and audible noise evaluation for different types of conductors.